

- Figure S1** Cyclic voltammograms of ligands and Ru-complexes (mM range in acetonitrile + NBu<sub>4</sub>PF<sub>6</sub> at 0.1M).  $v = 200 \text{ mV s}^{-1}$ .
- Figure S2** Absorption spectra of **L2** and of its model compound **L4** in dichloromethane.
- Figure S3** Frontier MO diagrams of **RuL1-3** complexes with main transitions.
- Figure S4** Simulated UV-Vis spectra of **L1-3** and **RuL1-3** for trans and cis isomers.
- Figure S5** Frontier MO of **L1-3** and **RuL1-3** complexes for cis isomers.
- Figure S6** Evolution of the absorption and luminescence spectra of **RuL1-3** upon irradiation at 436 nm. (solvent: degassed THF,  $\lambda_{\text{exc}} : 470 \text{ nm}$ ).
- Table S1** Computed amount of transferred charge and charge transfer distances of **L1-3** and **RuL1-3**.
- Table S2** Absorption maxima and corresponding shifts between ligand and complexes.
- Table S3** Computed photophysical data of **L1-3** and **RuL1-3** complexes for cis isomers.
- Methods** Experimental section (p. 2).  
Determination of photoisomerization quantum yields (p. 15).

## Experimental section

**Materials.** All reagents for synthesis were commercially obtained from Aldrich. All solvents for synthesis were dried and purified by standard procedures. The solvents used for absorption and emission analysis are as follows: Methylcyclohexane (MCH), Tetrahydrofuran (THF), Dichloromethane (DCM), Acetonitrile (ACN), Ethanol (EtOH). All the solvents employed were Aldrich or Fluka spectroscopic grade. Tris(2,2'-bipyridine)ruthenium(II) hexafluorophosphate, tetrabutylammonium hexafluorophosphate for electrochemical analysis were purchased from Aldrich.

**Physical Measurements and Instrumentation.** NMR spectra were recorded on AV 400 MHz or AV 500 MHz spectrometers.  $^1\text{H}$  and  $^{13}\text{C}$  chemical shifts are given versus  $\text{SiMe}_4$  and were determined by reference to residual  $^1\text{H}$  and  $^{13}\text{C}$  solvent signals. High resolution mass spectra (HRMS) were performed on a MS/MS ZABSpec TOF at the CRMPO (Centre de Mesures Physiques de l'Ouest) in Rennes.

The absorption measurements were carried out with a Perkin Elmer Lambda 2 double beam UV-vis spectrophotometers.

Steady-state luminescence spectra were collected from a FluoroMax-4 spectrofluorometer. Emission spectra are spectrally corrected from the instrument response. Phosphorescence measurements were performed in glassy matrix of ethanol at 77 K. The samples were placed in a 5-mm diameter quartz tube inside a Dewar filled with liquid nitrogen. Phosphorescence lifetimes were performed using the FluoroMax-4 spectrofluorometer which is also equipped with a Xe-pulsed lamp operating at up to 25 Hz. The time interval of the signal collection is initiated at a certain delay after a short exciting pulse so that the short-lived fluorescence (ns scale) can decay completely and phosphorescence becomes detectable. The

phosphorescence lifetimes are recorded according to a time-gated method. In this case the phosphorescence is recorded using a control module that includes a gate-and-delay generator which allows the integration of the signal during a specific period after a flash (delay) and for a pre-determined time window. The total signal is accumulated for a large number of exciting pulses.

The quantum yield measurements of the *trans*→*cis* photoisomerization ( $\Phi_{t\rightarrow c}$ ) were carried out under continuous irradiation at 436 nm with an Hg-Xe lamp (LC 9588/01A from Hamamatsu) equipped with a band pass filter centred at 440 nm (FB440-10 from Thorlabs). The progress of the reaction was monitored via the absorbance change at 436 nm (probe) using the transmitted actinide beam whose intensity was collected using a spectrometer (USB4000 from Ocean Optics). The intensity of the incident light ( $4.8 \times 10^{-7}$  einstein/min at 436 nm) was measured with the ferrioxalate actinometer.<sup>[1]</sup> Experiments were performed at 25°C in air equilibrated solutions which were continuously stirred. The detailed methodology for the calculation of  $\Phi_{t\rightarrow c}$  is detailed in Supporting Information. The experimental error on the quantum yield is estimated to be 10 %.

The cyclic voltammetry experiments <sup>[2]</sup> (using a computer-controlled Radiometer Voltalab 6 potentiostat with a three-electrode single-compartment cell; the working electrode was a platinum disk; a saturated calomel electrode (SCE) used as a reference was placed in a separate compartment) were performed at 300 K, in N<sub>2</sub>-degassed acetonitrile with a constant concentration (0.1 M) of n-Bu<sub>4</sub>BF<sub>4</sub>. Ferrocene was used as an internal reference.

**Computational methods.** To gain insight into the geometries and electronic properties of the studied ligands and complexes, Density Functional Theory (DFT)

computations were performed. The calculations reported in this work were performed using the Gaussian09 program.<sup>[3]</sup> The geometries of all the compounds have been optimized without symmetry constraints using the long-range separated hybrid functional CAM-B3LYP functional<sup>[4]</sup> and the Los Alamos effective core potential plus valence double zeta (LanI2dz)<sup>[5]</sup> basis set augmented with polarization functions on all atoms, except the hydrogen ones. DFT optimized geometries were confirmed as minima on the potential energy surfaces by calculations of the frequencies of the normal modes of vibration. Solvent effects, namely DCM (CH<sub>2</sub>Cl<sub>2</sub>), have been simulated by means of the polarizable continuum model (PCM).<sup>[6]</sup> Next, TD-DFT calculations have been performed at the same level of theory using the previously optimized geometries. In order to find the most appropriate computational model, some preliminary calculations were performed, different DFT functionals (MPW1PW91,<sup>[7]</sup> ωB97X,<sup>[8]</sup> PBE1PBE<sup>[9]</sup>) were tested, and the used computational model, i.e. CAM-B3LYP, was chosen for its consistency with experimental data.

**Synthetic procedures.** All manipulations were performed using Schlenk techniques under an Ar atmosphere. 5-Ethynyl-2,2'-bipyridine and **L4** were obtained as previously described.<sup>[10]</sup>

**(E)-4-((2-bromopyridin-4-yl)diazanyl)-N,N-dibutylaniline 2.** NaNO<sub>2</sub> (400 mg, 5.80 mmol) was added to a solution of 4-amino-2-bromopyridine (1g, 5.78 mmol) in 5 mL of HBF<sub>4</sub> (48% in H<sub>2</sub>O) at 0°C. The solution was vigorously stirred during 10 min, before dropwise addition of *N,N*-dibutylaniline (1.37 g, 11.56 mmol). The resulting mixture was stirred overnight at room temperature. Aqueous solution of NaOH (5 M) was added until neutralization. The crude product was extracted into DCM. The

organic phase was dried and solvents were evaporated. **2** was obtained as a red oil after column chromatography [SiO<sub>2</sub>, Pentane/CH<sub>2</sub>Cl<sub>2</sub> (1:3)]. **2** was used in the next reaction without further purification. (1.87 g, 83%). <sup>1</sup>H NMR (CDCl<sub>3</sub>, 400 MHz): δ = 8.43 (d, *J* = 5.3 Hz, 1H), 7.86 (d, *J* = 9.2 Hz, 2H), 7.80 (d, *J* = 1.5 Hz, 1H), 7.60 (dd, *J* = 5.3, 1.5 Hz, 1H), 6.69 (d, *J* = 9.2 Hz, 2H), 3.40 (t, *J* = 7.7 Hz, 4H), 1.64 (m, 4H), 1.40 (m, 4H), 0.99 ppm (t, *J* = 7.3 Hz, 6H).

**(E)-4-([2,2'-bipyridin]-4-yl diazenyl)-N,N-dibutylaniline L1.** 2-Bromopyridine (0.11 mL, 1.1 mmol) was drop-wisely added to a THF (10 mL) solution of *t*-BuLi (1.9 M in pentane, 1.2 mL, 2.28 mmol) at -78 °C. This mixture was maintained at -78 °C for 45 min. Then, anhydrous ZnCl<sub>2</sub> (370 mg, 2.8 mmol) in 10 mL THF was added slowly, and the reaction mixture was stirred for 2 h at room temperature. A THF solution (10 mL) of Pd<sub>2</sub>(dba)<sub>3</sub>·CHCl<sub>3</sub> (27 mg, 3 mol %), *t*-Bu<sub>3</sub>PH·BF<sub>4</sub> (18 mg, 6 mol %), and **2** (390 mg, 1.0 mmol) was then added. The yellow-orange reaction mixture was heated under reflux until the starting material had been consumed (Thin Layer Chromatography). After the mixture was cooled to room temperature, a suspension of EDTA (5 g, 17 mmol) in water (75 mL) was added, and the resulting mixture was stirred for 15 min. A saturated aqueous sodium bicarbonate solution was added until pH 8.0. The mixture was extracted several times with CH<sub>2</sub>Cl<sub>2</sub>, dried over Na<sub>2</sub>SO<sub>4</sub>, and the solvents were removed in vacuo. The pure product was obtained after column chromatography [SiO<sub>2</sub>, CH<sub>2</sub>Cl<sub>2</sub>/MeOH (99:1)], as a red oil (350 mg, 89%). <sup>1</sup>H NMR (CDCl<sub>3</sub>, 400 MHz): δ = 8.76 (d, *J* = 5.2 Hz, 1H), 8.73 (m, 2H), 8.43 (d, *J* = 7.9 Hz, 1H), 7.91 (d, *J* = 9.0 Hz, 2H), 7.82 (t, *J* = 7.5 Hz, 1H), 7.66 (d, *J* = 5.2 Hz, 1H), 7.31 (m, 1H), 6.69 (d, *J* = 9.0 Hz, 2H), 3.37 (m, 4H), 1.62 (m, 4H), 1.39 (m, 4H), 0.98 ppm (t, *J* = 7.3 Hz). <sup>13</sup>C {<sup>1</sup>H} NMR (CDCl<sub>3</sub>, 400 MHz): δ = 159.4, 157.7, 156.3, 151.6,

150.3, 149.3, 143.2, 136.8, 126.3, 123.7, 121.3, 115.9, 113.8, 111.1, 51.0, 29.5, 20.3, 14.0 ppm. MS (Zabspec-TOF):  $m/z$ : 410.2317 [ $M+Na^+$ ], 388.2505 [ $M+H^+$ ]; elemental analysis calcd (%) for  $C_{24}H_{29}N_5$ : C, 74.39; H, 7.54; N, 18.07; found: C, 74.59; H, 7.48; N, 17.80.

**4-(N,N-dibutylamino)-4'-iodoazobenzene 6.**  $NaNO_2$  (342 mg, 4.96 mmol) in 5 mL of water was added to the solution of 4-iodo-aniline (1 g, 4.57 mmol) in a diluted solution of HCl (2 mL HCl 37% in 18 mL of  $H_2O$ ), at 0 °C. After 20 min, a solution of N,N-dibutyl-aniline (1.03 g, 5.02 mmol) and  $NH_4OAc$  (130 mg, 1.69 mmol) in 10 mL of water and 25 mL of EtOH was added. The mixture was stirred during 2 days. After neutralization with  $NaHCO_3$ , the solution was extracted with  $CH_2Cl_2$  and washed several times with water. The pure product was obtained as a red solid (1.43 g, 72%), after column chromatography [ $SiO_2$ , Pentane/ $CH_2Cl_2$  (7:3)]  $^1H$  NMR (400 MHz,  $CDCl_3$ ):  $\delta$  = 7.83 (d,  $J$  = 9.1 Hz, 2H), 7.79 (d,  $J$  = 8.5 Hz, 2H), 7.56 (d,  $J$  = 8.5 Hz, 2H), 6.68 (d,  $J$  = 9.1 Hz, 2H), 3.36 (m, 4H), 1.62 (m, 4H), 1.39 (m, 4H), 0.98 ppm (t,  $J$  = 7.3 Hz, 6H).  $^{13}C$  { $^1H$ } NMR (100 MHz,  $CDCl_3$ ):  $\delta$  = 152.6, 150.9, 142.9, 138.1, 125.5, 123.9, 111.2, 94.9, 51.0, 29.5, 20.3, 14.0 ppm. MS (Zabspec-TOF):  $m/z$ : 436.1247 [ $M+H^+$ ], 435.1171 [ $M^+$ ]; elemental analysis calcd (%) for  $C_{20}H_{26}N_3I$ : C, 55.18; H, 6.02; N, 9.65; found: C, 55.61; H, 6.03; N, 9.62.

**5-(1-(4-(N,N-dibutylamino)-4'-azobenzene)-ethynyl)-2,2'-bipyridine (L2).** 5-(ethynyl)-2,2'-bipyridine (100 mg, 0.55 mmol) and 4-(N,N-dibutylamino)-4'-iodoazobenzene (240 mg, 0.55 mmol) were dissolved in 30 mL of freshly distilled triethylamine, and placed under argon.  $CuI$  (10 mg, 0.053 mmol) and  $Pd(PPh_3)_2Cl_2$  (17 mg, 0.027 mmol) were added to the mixture. The solution was heated at 50 °C

during 2 days. Solvent was evaporated. 20 mL of CH<sub>2</sub>Cl<sub>2</sub> and 50 mL of an aqueous saturated solution of EDTA were added. The mixture was vigorously stirred for 2h. Phases were separated and the organic phase was washed two times with water. Solvents were evaporated. The crude product was subjected to a column chromatography on silica gel, with CH<sub>2</sub>Cl<sub>2</sub>/MeOH (2%) as eluent and obtained as a red solid (130 mg, 48%). <sup>1</sup>H NMR (400 MHz, CD<sub>2</sub>Cl<sub>2</sub>) : δ = 8.85 (s, 1H), 8.70 (d, *J* = 3.3 Hz, 1H), 8.48 (d, 1H), 8.48 (d, 1H), 7.98 (d, *J* = 8.1 Hz, 1H), 7.86 (d, 2H), 7.86 (d, 1H), 7.86 (d, 2H), 7.70 (d, *J* = 7.9 Hz, 2H), 7.35 (m, 1H), 6.75 (d, *J* = 8.6 Hz, 2H), 3.40 (m, 4H), 1.66 (m, 4H), 1.42 (m, 4H), 1.01 ppm (t, *J* = 7.2 Hz, 6H). <sup>13</sup>C {<sup>1</sup>H} NMR (100 MHz, CD<sub>2</sub>Cl<sub>2</sub>) : δ = 155.3, 154.9, 153.1, 151.5, 151.0, 149.2, 143.0, 139.2, 136.8, 132.4, 125.4, 123.9, 122.9, 122.2, 121.1, 120.2, 120.1, 111.1, 93.5, 87.9, 50.9, 29.4, 20.2, 13.7 ppm. MS (Zabspec-TOF): *m/z*: 510.2632 [*M*+Na<sup>+</sup>], 488.2810 [*M*+H<sup>+</sup>]; elemental analysis calcd (%) for C<sub>32</sub>H<sub>33</sub>N<sub>5</sub>: C, 78.82; H, 6.82; N, 14.36; found: C, 78.61; H, 6.73; N, 14.26.

### **5-(1-(4-(N,N-dibutylamino)-4'-azobenzene)-1*H*-1,2,3-triazol-4-yl)-2,2'-bipyridine**

**(L3).** 4-(N,N-dibutylamino)-4'-iodoazobenzene (218 mg, 0.6 mmol) was mixed with 5-(ethynyl)-2,2'-bipyridine (90 mg, 0.5 mmol, 1 equiv). To this mixture were successively added L-proline (12 mg, 0.1 mmol, 0.2 equiv), Na<sub>2</sub>CO<sub>3</sub> (12 mg, 0.1 mmol, 0.2 equiv), NaN<sub>3</sub> (39 mg, 1 mmol, 2 equiv), sodium ascorbate (20 mg, 0.05 mmol, 0.1 equiv), 1 mL 9:1 DMSO/H<sub>2</sub>O, and CuSO<sub>4</sub>·5H<sub>2</sub>O (13 mg, 0.025 mmol, 0.05 equiv). The mixture was stirred overnight at 65 °C. Upon completion (monitored by TLC), the crude mixture was poured into 30 mL of saturated aqueous solution of EDTA and stirred during 30 min. The red precipitate was isolated by filtration and washed with dilute NH<sub>4</sub>OH (CAUTION: this step is important, as copper azides are

explosive when dry, and their traces should be removed before the product is dried). The crude product was dissolved in  $\text{CH}_2\text{Cl}_2$  and subjected to a column chromatography on silica gel, first with  $\text{CH}_2\text{Cl}_2$  (remove starting materials), then ethyl acetate. The product was obtained as a red solid (191 mg, 72%).  $^1\text{H}$  NMR (400 MHz,  $\text{CDCl}_3$ ):  $\delta$  = 9.20 (s, 1H), 8.72 (d,  $J$  = 4.4 Hz, 1H), 8.52 (d,  $J$  = 8.3 Hz, 1H), 8.46 (d,  $J$  = 7.9 Hz, 1H), 8.39 (d,  $J$  = 8.3 Hz, 1H), 8.36 (s, 1H), 8.01 (d,  $J$  = 8.5 Hz), 7.91 (d,  $J$  = 8.5 Hz, 2H), 7.87 (d,  $J$  = 9.0 Hz, 2H), 7.83 (d,  $J$  = 7.8 Hz, 1H), 7.33 (dd,  $J$  = 6.6, 5.4 Hz, 1H), 6.70 (d,  $J$  = 8.7 Hz, 2H), 3.38 (t,  $J$  = 7.6 Hz, 4H), 1.63 (m, 4H), 1.40 (m, 4H), 0.99 ppm (t,  $J$  = 7.2 Hz, 6H).  $^{13}\text{C}$   $\{^1\text{H}\}$  NMR (100 MHz,  $\text{CDCl}_3$ ):  $\delta$  = 155.9, 155.7, 153.3, 151.1, 149.3, 146.6, 145.4, 143.0, 137.0, 136.6, 134.0, 126.2, 125.7; 123.9, 123.5, 121.2, 121.2, 121.0, 118.0, 111.1, 51.0, 29.5, 20.3, 14.0 ppm. MS (Zabspec-TOF):  $m/z$ : 553.2804 [ $M+\text{Na}^+$ ], 525.2747 [ $M-\text{N}_2+\text{Na}^+$ ]; elemental analysis calcd (%) for  $\text{C}_{32}\text{H}_{34}\text{N}_8$ , EtOAc: C, 71.49; H, 6.60; N, 20.01; found: C, 71.30; H, 6.36; N, 20.31.



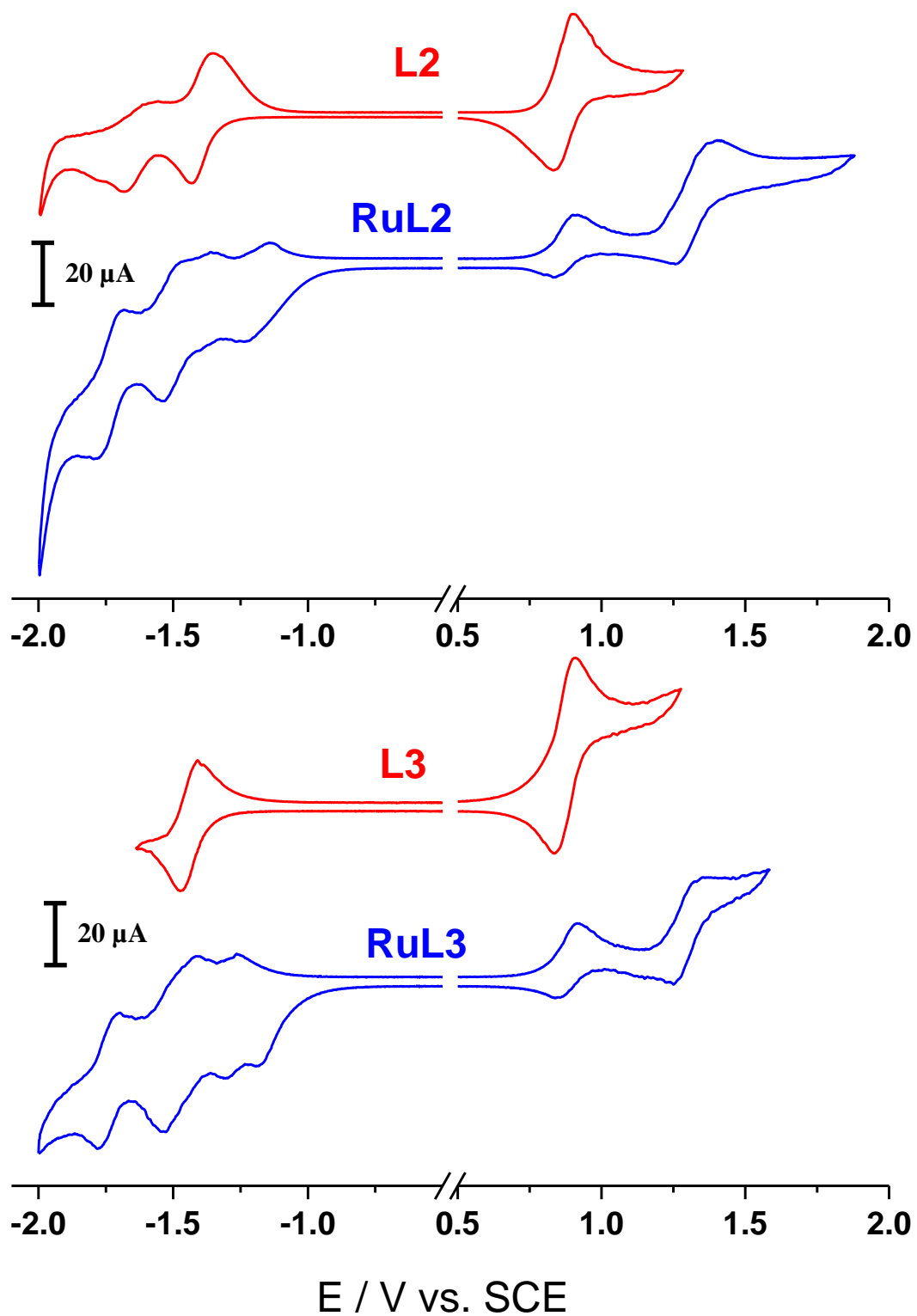


**Figure S1.** Cyclic voltammograms of ligands and Ru-complexes (mM range in acetonitrile NBu<sub>4</sub>PF<sub>6</sub> at 0.1M).  $\nu = 200 \text{ mV s}^{-1}$ .

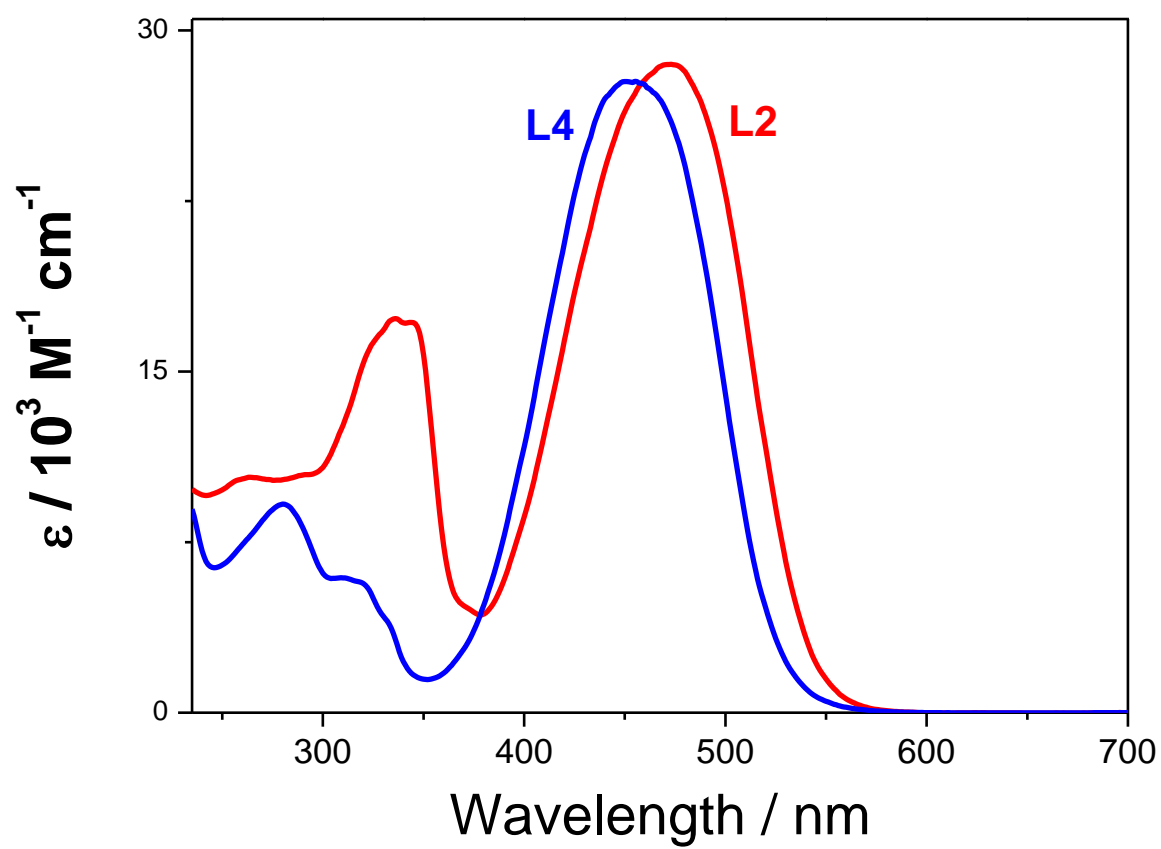


**Figure S2.** Absorption spectra of **L2** and of its model compound **L4** in dichloromethane.

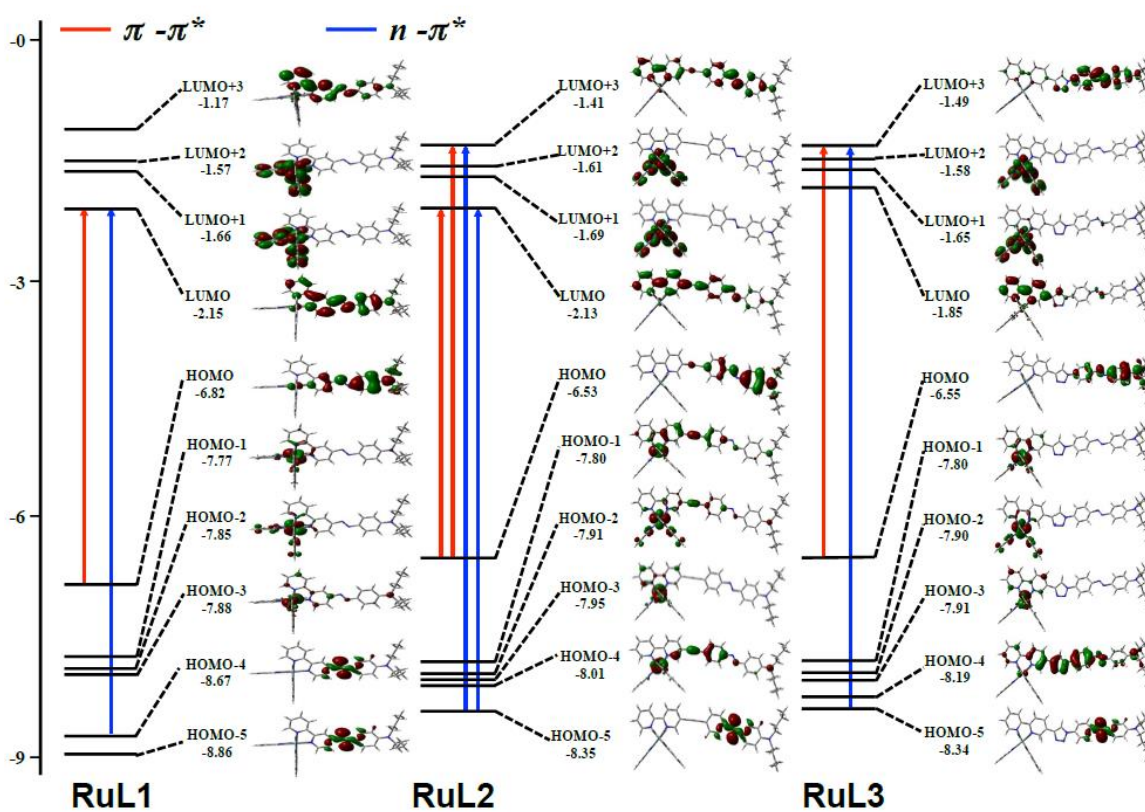
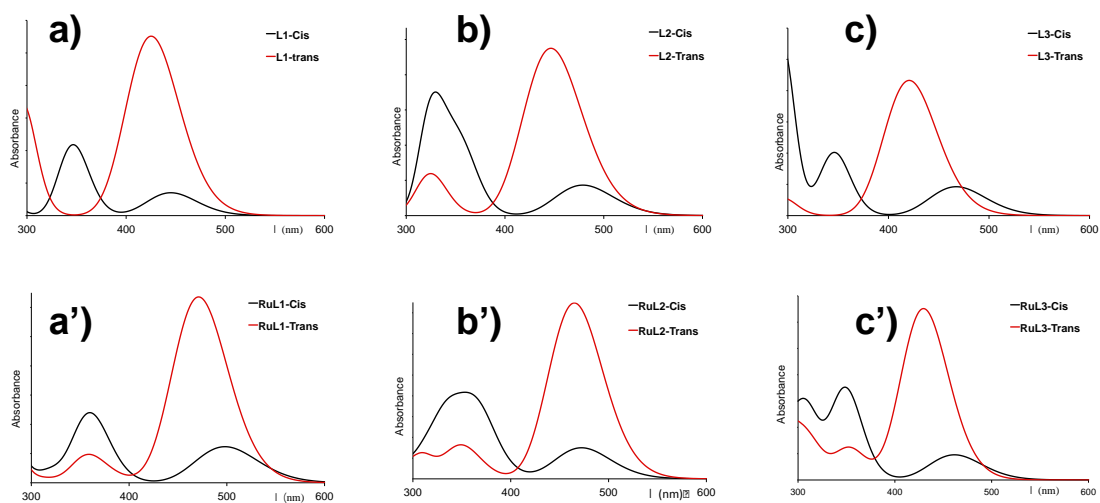


Figure S3. Frontier MO diagrams of RuL1-3 complexes with main transitions.



**Figure S4.** Comparison of simulated UV-Vis absorption spectra at the CAM-B3LYP/ LANL2DZP level in  $\text{CH}_2\text{Cl}_2$  for trans and cis isomers: (a) **L1**, (b) **L2**, (c) **L3**, (a') **RuL1**, (b') **RuL2**, and (c') **RuL3**.

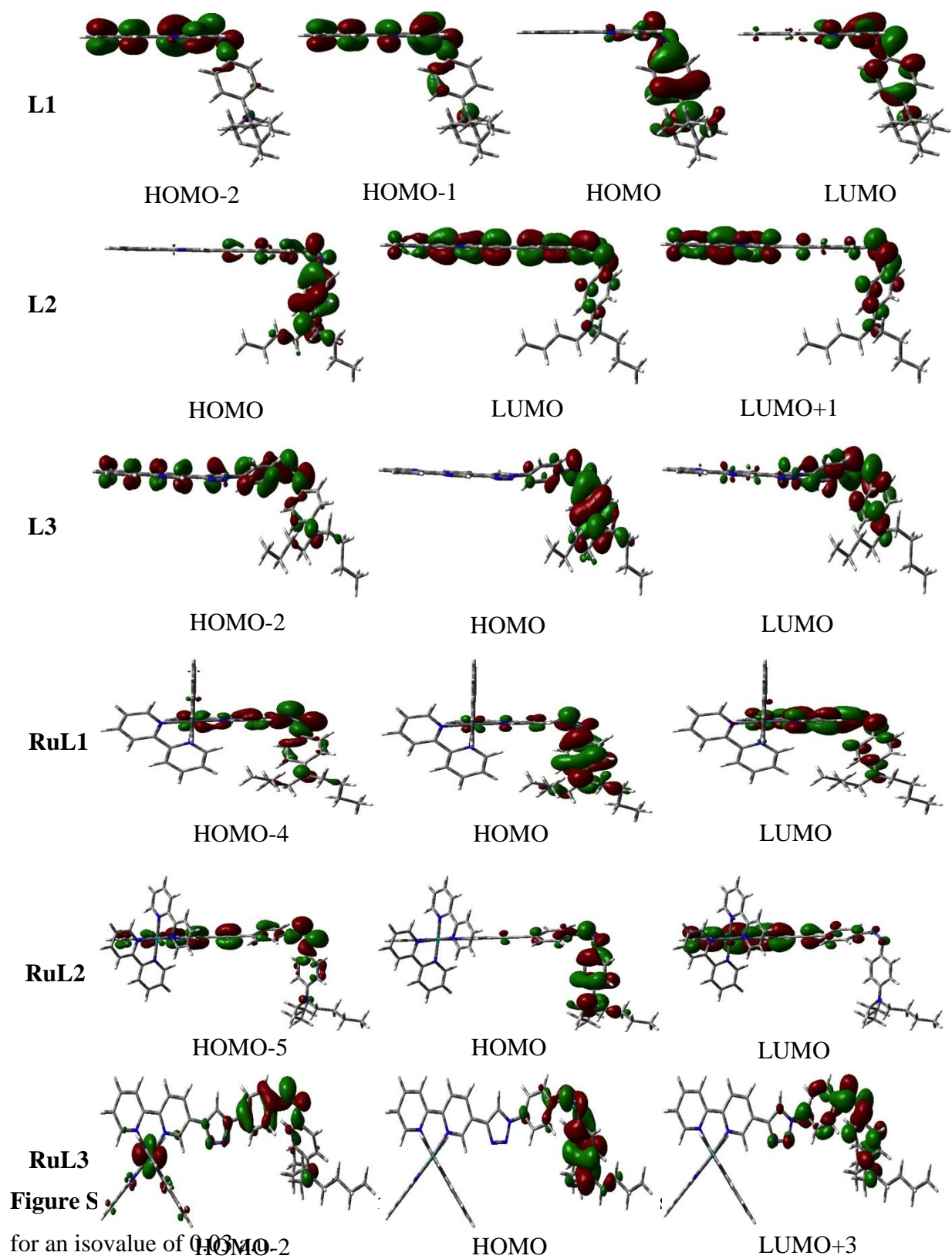
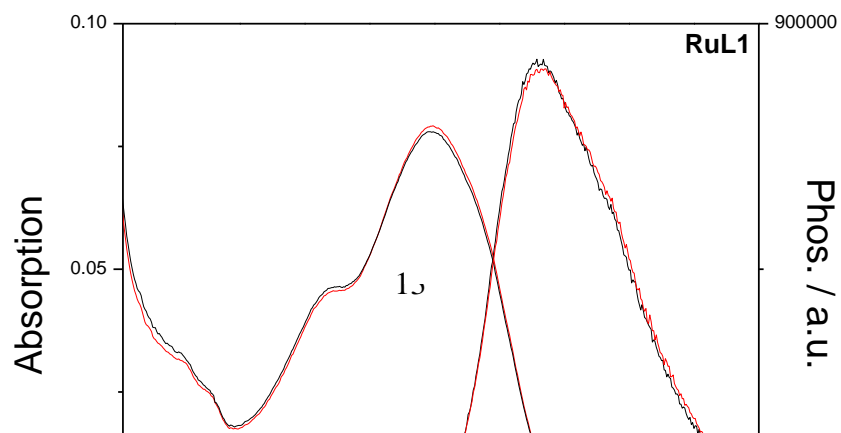


Figure S1

for an isovalue of 0.05



**Figure S6** Evolution of the absorption and luminescence spectra of **RuL1-3** upon irradiation at 436 nm. (solvent: degassed THF,  $\lambda_{\text{exc}}$  : 470 nm).

**Table S1.** Amount of transferred charge ( $q^{\text{CT}}$ ) and charge transfer distances ( $d^{\text{CT}}$ ) computed for ligands and complexes in  $\text{CH}_2\text{Cl}_2$  at CAM-B3LYP/LANL2DZP level.

Assignment	<b>L1</b>		<b>RuL1</b>		
	$q^{CT}$ (e)	$d^{CT}$ (Å)	$q^{CT}$ (e)	$d^{CT}$ (Å)	
$S_1 - S_0$ (n- $\pi^*$ )	0.73	0.30	$S_1 - S_0$ ( $\pi$ - $\pi^*$ )	0.58	2.50
$S_2 - S_0$ ( $\pi$ - $\pi^*$ )	0.58	3.13	$S_2 - S_0$ (n- $\pi^*$ )	0.76	0.16
	<b>L2</b>		<b>RuL2</b>		
$S_1 - S_0$ ( $\pi$ - $\pi^*$ )	0.56	2.90	$S_1 - S_0$ ( $\pi$ - $\pi^*$ )	0.61	4.34
$S_2 - S_0$ (n- $\pi^*$ )	0.73	0.10	$S_2 - S_0$ (n- $\pi^*$ )	0.74	0.17
	<b>L3</b>		<b>RuL3</b>		
$S_1 - S_0$ (n- $\pi^*$ )	0.73	0.14	$S_1 - S_0$ (n- $\pi^*$ + $\pi$ - $\pi^*$ )	0.57	1.20
$S_2 - S_0$ ( $\pi$ - $\pi^*$ )	0.57	2.90	$S_2 - S_0$ ( $\pi$ - $\pi^*$ + n- $\pi^*$ )	0.57	1.89

**Table S2.** Experimental (Exp.) and calculated (Calc.) absorption maxima (eV) and corresponding shifts between ligand and complex ( $\Delta$ , eV) for trans isomers.

	<b>L1</b>		<b>L2</b>		<b>L3</b>	
	Exp.	Cal.	Exp.	Cal.	Exp.	Cal.
Ligand ( <b>L</b> )	2.70	2.95	2.63	2.78	2.68	2.92
Complex ( <b>RuL</b> )	2.17	2.63	2.55	2.66	2.70	2.89
$\Delta$ ( <b>L-RuL</b> )	0.53	0.32	0.08	0.12	-0.02	0.03

**Table S3.** Computed absorption wavelengths  $\lambda_{Calc.}$  (nm) ( $\Delta E$  (eV)), oscillator strengths ( $f$ ) and main transitions of cis isomers in  $CH_2Cl_2$  at the CAM-B3LYP/Lan12DZP level.

	$\lambda_{Calc.}$ (nm) ( $\Delta E$ (eV))	$f$	Main transitions (% weight)
n- $\pi^*$	445 (2.78)	0.19	HOMO->LUMO(+41%) HOMO-1->LUMO(27%) HOMO-2->LUMO(21%)
n- $\pi^*$	479 (2.60)	0.36	HOMO->LUMO(+39%) HOMO->LUMO+1(20%)
n- $\pi^*$	467 (2.65)	0.25	HOMO->LUMO(+50%) HOMO-2->LUMO(22%)
n- $\pi^*$	498 (2.49)	0.34	HOMO->LUMO(+50%) HOMO-4->LUMO(+18%)
n- $\pi^*$	472 (2.62)	0.41	HOMO->LUMO+3(+39%) HOMO-5->LUMO+3(+14%)
n- $\pi^*$	461 (2.69)	0.26	HOMO->LUMO+3(+48%) HOMO-2->LUMO+3 (+16%)

### Determination of photoisomerization quantum yields.

The quantum yield measurements of the *trans*→*cis* photoisomerization were carried out under continuous irradiation at 436 nm with an Hg-Xe lamp (LC 9588/01A from Hamamatsu)

equipped with a band pass filter centred at 440 nm (FB440-10 from Thorlabs). The progress of the reaction (see **Figure S6**) was monitored via the absorbance change at 436 nm using the transmitted actinide beam whose intensity was collected using a spectrometer (USB4000 from Ocean Optics). The intensity of the incident light ( $4.8 \times 10^{-7}$  einstein/min at 436 nm) was measured with the ferrioxalate actinometer<sup>[1]</sup>. Experiments were performed at 25°C in air equilibrated solutions which were continuously stirred.

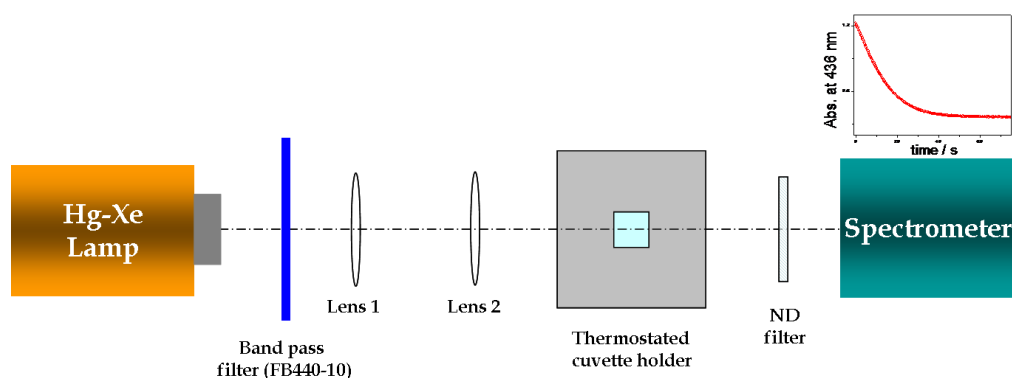
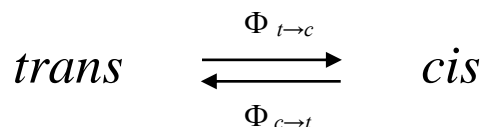


**Figure S7.** Setup for photochemical quantum yield measurement.



Initial condition ( $t = 0$ )       $C_0$

Stationary state ( $t \rightarrow \infty$ )       $C_0 - x$                        $x$

According to the formalism proposed by Michl *et al.*<sup>[11]</sup>, the absorption time dependence relationship of a chromophore *trans* which undergoes a photochemical interconversion *trans*  $\leftrightarrow$  *cis* can be expressed as follows:

$$g(t) = A(t) - A_0 + A_\infty \ln \frac{A(t) - A_\infty}{A_0 - A_\infty} = -\frac{l}{V} \cdot \Phi \cdot \left[ \int_0^t F(t) dt - \int_0^t F(t) \cdot 10^{-A(t)} dt \right] \quad (1)$$

In this equation,  $A_0$  and  $A_\infty$  denote the absorbances before irradiation and at the photostationary state respectively.  $F(t)$ ,  $V$ ,  $l$  are the total incident photon flux, the irradiation volume in the cell and the optical path. Finally  $\Phi$  represents the weighted sum of the two photoisomerization quantum yields:

$$\Phi = \varepsilon_{tr} \cdot \Phi_{t \rightarrow c} + \varepsilon_{cis} \cdot \Phi_{t \rightarrow c} \quad (2)$$

where  $\varepsilon_{tr}$  and  $\varepsilon_{cis}$  represent the extinction coefficients of each species at  $\lambda_{irr}$ . The relation 2 can be rewritten in the form given in equation 3:



$$\Phi = \frac{\varepsilon_{tr} \cdot \Phi_{t \rightarrow c}}{f_{cis}(\infty)} = \frac{\varepsilon_{cis} \cdot \Phi_{c \rightarrow t}}{f_{tr}(\infty)} \quad (3)$$

We define  $f_{tr}(\infty)$  and  $f_{cis}(\infty)$  as the molar fractions of the photoisomers at the photostationary state. Therefore the calculation of the *trans-to-cis* photoisomerization quantum yield requires the experimental determination of  $\Phi$ ,  $\varepsilon_{tr}$  and  $f_{cis}(\infty)$ .

If the photon flux is constant,  $F(t) = K$ , and the absorbance of the irradiated solution is sufficiently high (i.e.  $10^{-A(t)} \approx 0$ ), the equation 1 can be simplified as follows :

$$g(t) \approx -\frac{IK}{V} \cdot \Phi \cdot t \quad (4)$$

This linearization method holds true if we also consider that the *cis-to-trans* thermal reaction can be neglected at the initial step of the irradiation. From a practical point of view, the linear approximation has considered in time scale far below the half-life time of this thermal reaction (ie  $\tau_{1/2}$ ). **Figure S7** typically displays such a linearization method. It should be noted that the azobenzene in cyclohexane was used as actinometer<sup>[1, 12]</sup> (i.e.  $\Phi_0 = \varepsilon_{tr}^0 \cdot \Phi_{tr} + \varepsilon_{cis}^0 \cdot \Phi_{cis}$  with  $\varepsilon_{tr}^0 = 510 \text{ M}^{-1} \text{ cm}^{-1}$ ,  $\varepsilon_{cis}^0 = 1520 \text{ M}^{-1} \text{ cm}^{-1}$ ,  $\Phi_{tr} = 0.28$ ,  $\Phi_{cis} = 0.55$  at  $\lambda_{irr} : 436 \text{ nm}$ ).

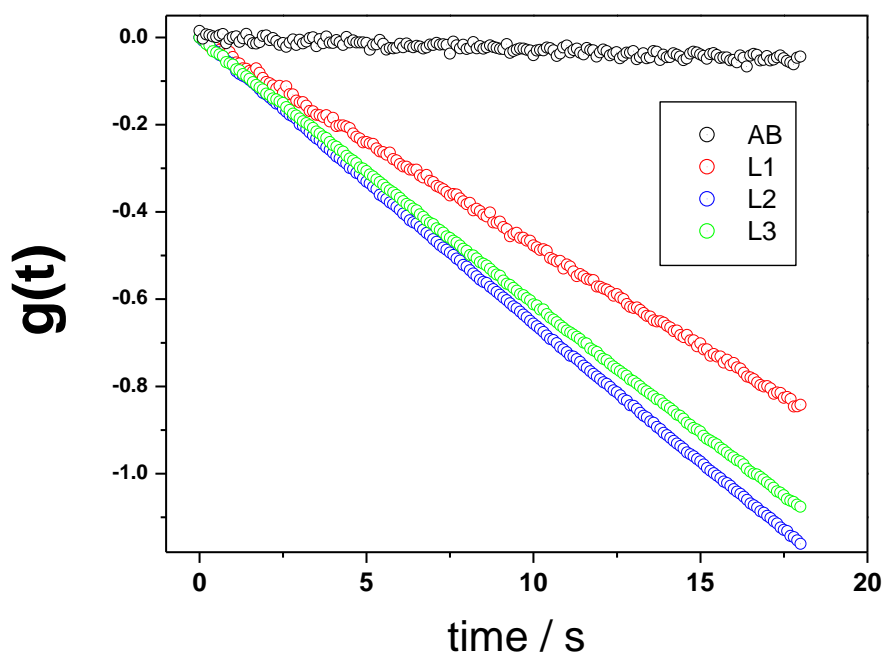


**Figure S8.** Quantum yield determination of the *trans-to-cis* photoisomerization of L1-3 in MCH upon excitation at 436 nm. Azobenzene (AB) in cyclohexane is used as actionometer. Finally, the molar fraction of *cis* isomer,  $f_{tr}(\infty)$ , at photostationary state has been evaluated spectrometrically according to the change of the absorbance at maximum absorption wavelength of the *trans* isomer as follows:

$$f_{cis}(\infty) = \frac{A_0^{MAXtr} - A_\infty^{MAXtr}}{A_0^{MAXtr}} \cdot \frac{\epsilon_r^{MAXtr}}{\epsilon_r^{MAXtr} - \epsilon_{cis}^{MAXtr}} \approx \frac{A_0^{MAXtr} - A_\infty^{MAXtr}}{A_0^{MAXtr}}$$

In this case, we assume that  $\epsilon_r^{MAXtr} \gg \epsilon_{cis}^{MAXtr}$  which was clearly corroborated by the TD-DFT simulated absorption spectra of each isomer.

## References.

- [1] M. Montalti, A. Credi, L. Prodi and M. T. Gandolfi, *Handbook of Photochemistry, Third Ed.*, CRC Press, Boca Raton, **2006**.
- [2] J. P. Malval, J. P. Morand, R. Lapouyade, W. Rettig, G. Jonusauskas, J. Oberle, C. Trieflinger and J. Daub, *Photochem. Photobiol. Sci.* **2004**, *3*, 939-948.
- [3] M. Frisch, G. Trucks, H. Schlegel, G. Scuseria, M. Robb, J. Cheeseman, G. Scalmani, V. Barone, B. Mennucci, G. Petersson, H. Nakatsuji, M. Hada, M. Ehara, K. Toyota, R. Fukuda, J. Hasegawa, M. Ishida, T. Nakajima, Y. Honda, O. Kitao, H. Nakai, M. Klene, X. Li, J. Knox, H. Hratchian, J. Cross, V. Bakken, C. Adamo, J. Jaramillo, R. Gomperts, R. Stratmann, O. Yazyev, A. Austin, R. Cammi, C. Pomelli, J. Ochterski, P. Ayala, K. Morokuma, G. Voth, P. Salvador, J. Dannenberg, V. Zakrzewski, S. Dapprich, A. Daniels, M. Strain, O. Farkas, D. Malick, A. Rabuck, K. Raghavachari, J. Foresman, J. Ortiz, Q. Cui, A. Baboul, S. Clifford, J. Cioslowski, B. Stefanov, G. Liu, A. Liashenko, P. Piskorz, I. Komaromi, R. Martin and D. Fox *Gaussian 09, Revision D. 01*, Gaussian Inc, Wallingford CT, **2013**.
- [4] T. Yanai, D. P. Tew and N. C. Handy, *Chem. Phys. Lett.* **2004**, *393*, 51-57.
- [5] P. J. Hay and W. R. Wadt, *J. Chem. Phys.* **1985**, *82*, 299-310.
- [6] J. Tomasi, B. Mennucci and R. Cammi, *Chem. Rev.* **2005**, *105*, 2999-3094.
- [7] J. P. Perdew and Y. Wang, *Phys. Rev. B* **1992**, *45*, 13244.
- [8] J.-D. Chai and M. Head-Gordon, *J. Chem. Phys.* **2008**, *128*, 084106.
- [9] a) J. P. Perdew, K. Burke and M. Ernzerhof, *Phys. Rev. Lett.* **1996**, *77*, 3865; b) J. P. Perdew, M. Ernzerhof and K. Burke, *J. Chem. Phys.* **1996**, *105*, 9982-9985.
- [10] a) K. N. Gherab, R. Gatri, Z. Hank, B. Dick, R.-J. Kutta, R. Winter, J. Luc, B. Sahraoui and J.-L. Fillaut, *J. Mater. Chem.* **2010**, *20*, 2858-2864; b) A. M. Soliman, D. Fortin, P. D. Harvey and E. Zysman-Colman, *Chem. Commun.* **2012**, *48*, 1120-1122.
- [11] J. Tonne, H. Prinzbach and J. Michl, *Photochem. Photobiol. Sci.* **2002**, *1*, 105-110.
- [12] P. P. Birnbaum, J. H. Linford and D. W. G. Style, *Trans. Faraday Soc.* **1953**, *49*, 735-744.